EFFECTS OF PROJECTILE DEFORMATION ON CRATERING EFFICIENCY AND MORPHOLOGY. P. H. Schultz, Lunar and Planetary Institute, 3303 NASA Road 1, Houston, TX 77058 and Donald E. Gault, Murphys Center of Planetology, Box 833, Murphys, CA 95247.

INTRODUCTION: Theoretical calculations of cratering typically focus on very high velocity impacts where hydrodynamic behavior of the projectile and target is assured, whereas limitations in launch techniques restrict experimental studies to small projectiles (< 0.6 cm) and modest velocities (< 7 km/s). Most experimental studies concerned with energy-scaling relations use low-strength targets (e.g., sand) in order to simulate the hydrodynamic behavior of shock-induced strengthless targets produced by much larger and faster impacts. Although, this approach is valid for many applications, it generally ignores important changes in the cratering process as peak shock pressures increase. We report here experimental results that show significant differences in cratering efficiency between high and low velocity impacts that can be related to deformation/disruption of the projectile above a critical velocity. Projectile deformation is further shown to influence crater morphology for large projectiles with low velocities, thereby having implications for problems in planetary cratering.

Cratering Efficiency: Cratering efficiency (displaced-target-mass/projectile-mass) for a given gravity field, target, and projectile (size and mass) depends on kinetic energy. Schmidt and Holsapple (1) suggest that cratering efficiency depends more generally on gravity (g), impact velocity (v), and projectile radius (r) that are collectively expressed in dimensionless form as $\pi_2 = 3.22\ gr/v^2$. They observe that this dependence follows a single power-law relation over many orders of magnitude, thereby justifying application over broad ranges in component variables. Gault and Wedekind (2), however, noted that the relation between crater diameter and kinetic energy is better described by two separate power-law exponents -- a result consistent with impacts into metals (3). Figure 1a illustrates this transition (at velocities 1.5 - 2km/s) in cratering efficiency as a function of $\pi_2$ for 0.318 cm-diameter aluminum spheres impacting No. 24 sand under vacuum conditions (< 5 mm, Hg). The transition for 0.635 cm projectiles occurs over the same velocity range. Figure 1b further documents the transition by the progressive steepening of the power-law slope in Figure 1a as a function of impact velocity for 0.318 cm aluminum projectiles. Changes in slope also occur for pyrex and lexan projectiles, but at lower impact velocities (1.0 km/s). Recovered projectiles are deformed or disrupted as velocities approach and exceed values corresponding to these changes in power-law slope. Aluminum projectiles (0.318 cm diameter) impacting sand begin to deform on one side at 0.5 km/s, are flattened by 1.0 km/s, form a cup by 2.0 km/s, and are fragmented at 2.8 km/s. Above 1.3 km/s, the projectile is severely deformed with a diameter increase 1.7 fold. Pyrex projectiles of the same size begin to spall at 0.15 km/s, leave a cylindrical plug above 0.25 km/s, and are completely comminuted above 1 km/s.

These results suggest that cratering efficiency as a function of either kinetic energy or $\pi_2$ does not follow a single relation for sand targets but changes where the peak shock stresses exceed the dynamic strength of the projectile. Thus extrapolation to conditions outside the appropriate velocity region must be made with caution, and extrapolations to planet-scale events without consideration for projectile deformation should be revised.

Crater Morphology: Because the observed transitions in cratering efficiency occur at relatively low velocities where changes of state do not occur, we can explore other effects of projectile deformation with large objects using the Ames air gun. Systematic changes in aspect ratio (diameter/depth) and morphology are observed as a function of projectile strength, radius, and velocity, density and strength for a given target. For a projectile of given size, density, and strength impacting a given sand or pumice target, the aspect ratio increases slightly with increasing velocity as the peak shock pressures exceed the dynamic strength of the projectile. For a given projectile size, density, and velocity (and target), the aspect ratio increases with decreasing projectile strength. For strengthless projectiles (clustered impactors) with a given velocity (and target), the aspect ratio increases with increasing projectile size or decreasing density (4). Combining these independent variables as $\eta = (2r/v) \cdot (\delta_t/\delta_p) \cdot (S_t/S_p)$ provides a functional relation with the aspect ratio ($r$ = projectile radius; $v$ = impact velocity; $\delta_t$ and $\delta_p$, the density of the target and projectile, respectively; $S_t$ and $S_p$, the strength of the target and projectile, respectively). Figure 2 shows results for impacts into compacted pumice, a target that has greater strength than sand (identical trends occur in sand targets). The independent strength variable has not been included, but qualitative corrections account for seemingly disparate data (points B and D).

Figure 2 also illustrates a systematic change in crater morphology with $\eta$. Small values produce craters with a central pit. Intermediate values progressively change the floor profile from bowl shaped to mounded, whereas large values of $\eta$ produce flat floors with incipient rings.

The selection of $(2r/v)$ in $\eta$ is based on consistency with available data. It also can be understood physically as the time required for complete transfer of momentum from a strengthless projectile to the target. One-dimensional shock geometry shows that the reflected shock wave reaches the backside of a solid projectile before penetrating the surface for velocities less than 7 km/s for basalt/granite projectiles. Consequently, projectiles impacting at velocities high enough for tensile/plastic failure but below about 5 km/s can be considered -- to first order -- as fragmented and deformed objects before they get below the target surface. Future experiments and theory will be used to establish a physically meaningful dimensionless form of $\eta$.

In summary, projectile failure at low velocities (< 3 km/s) affects crater scaling relations, thereby dictating caution in applying certain laboratory results to high-velocity conditions or broad scales where projectile deformation occurs. Moreover, the combined effects of low to modest velocities and large projectile sizes may contribute to the distinctive crater interior morphologies on the Moon, Mars, and the Galilean/Saturnian satellites in addition to impact melting (5) and oscillations of a strengthless target (6).

# PROJECTILE DEFORMATION

P. H. Schultz and D. E. Gault

## References

1.) Schmidt R.M. and Holsapple K.A. (1980), J. Geophys. Res. 85, p. 235-252. 2.) Gault D.E. and Wedekind J. (1977), Impact and Explosion Cratering, D.J. Roddy et al. (eds.), p. 1231-1234. 3.) Summers J.L. (1959) NASA Tech. Note D-94. 4.) Schultz P.H. and Gault D.E. (1983), Lunar and Planetary Science XIV, p. 674-675, Lunar and Planetary Institute, Houston. 5.) Croft S.K. (1983) Lunar and Planetary Science XIV, p. 138-139, Lunar and Planetary Institute, Houston. 6.) Greeley R. (1982) in Satellites of Jupiter (D. Morrison, ed.) p. 340-378.

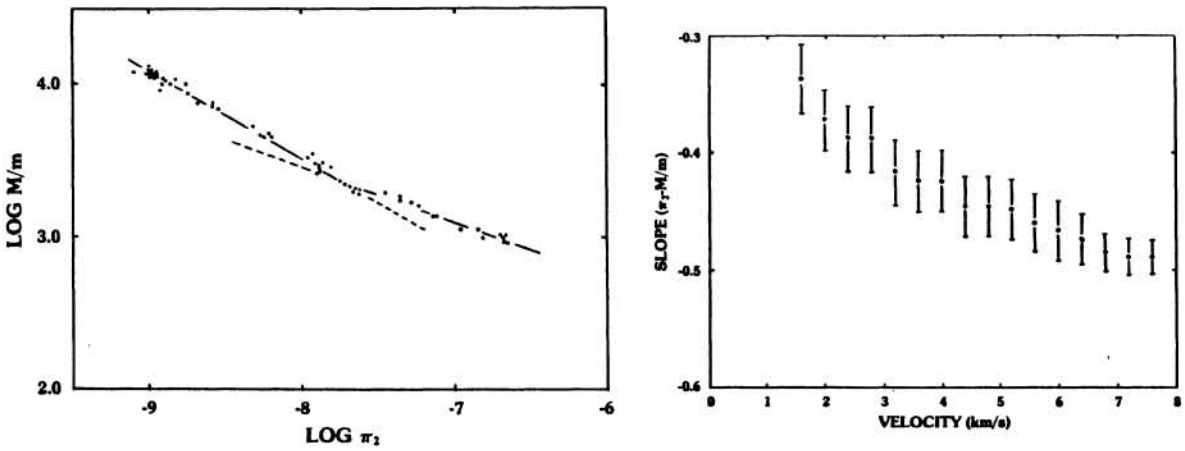


Figure 1. Displaced mass ratio as a function of the dimensionless $\Pi_2$ variable for constant size aluminum spheres (0.318 cm) impacting No. 24 sand (Fig. 1a). A change in slope occurs as the shock pressures exceed the compressive strength of aluminum at $\Pi_2$ values corresponding to velocities between 1.5 and 2 km/s.

Figure 1b shows the slope of the data in Fig. 1a for a progressively increasing minimum value of $\eta$ corresponding to an increasing minimum value of velocity. The slope clearly becomes steeper with increasing velocity (error bars indicate the 95% confidence level for the slope value).

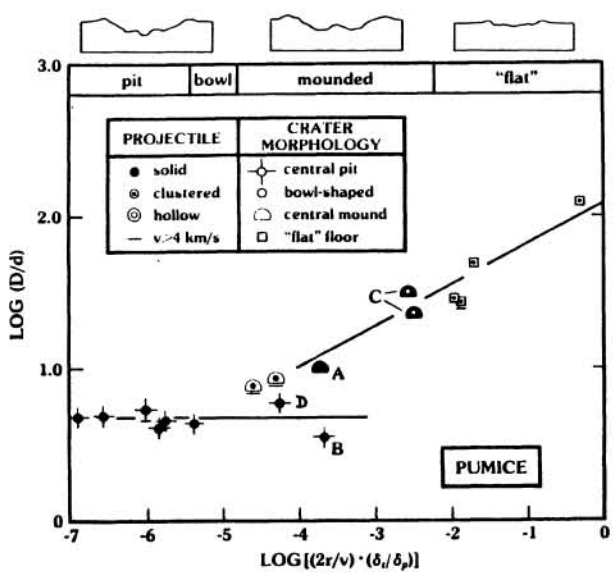


Figure 2. The change in aspect ratio (diameter/depth) as a function of penetration time (2r/v) and density ratio ($\delta_t / \delta_p$). As the time of penetration increases, the crater becomes shallower and exhibits changes in morphology as shown at top. Previous laboratory experiments consider values of log (2r/v) . ($\delta_t / \delta_p$) less than -5. Data points A and B correspond to identical size solid projectiles with very low strength and high strength, respectively. Data C and D indicate hollow and nylon spheres, respectively. Open symbols indicate impacts by clustered impactors with different dispersions.